

## DEVELOPMENT AND VERIFICATION OF A HIGH-PRECISION LASER MEASUREMENT SYSTEM FOR STRAIGHTNESS AND PARALLELISM MEASUREMENT

**Peng Xu<sup>1)</sup>, Rui Jun Li<sup>1)</sup>, Wen Kai Zhao<sup>1)</sup>, Zhen Xin Chang<sup>1)</sup>, Shao Hua Ma<sup>1)</sup>, Kuang Chao Fan<sup>1,2)</sup>**

1) *Hefei University of Technology, School of Instrument Science and Opto-Electronics Engineering, Hefei, China*  
([pengxu@mail.hfut.edu.cn](mailto:pengxu@mail.hfut.edu.cn), [rj-li@hfut.edu.cn](mailto:rj-li@hfut.edu.cn), +86 138 5697 1653, [zhaowk@mail.hfut.edu.cn](mailto:zhaowk@mail.hfut.edu.cn),  
[changzhenxin@mail.hfut.edu.cn](mailto:changzhenxin@mail.hfut.edu.cn), [shaohuama@mail.hfut.edu.cn](mailto:shaohuama@mail.hfut.edu.cn))

2) *Dalian University of Technology, School of Mechanical Engineering, Dalian, China* ([fan@ntu.edu.tw](mailto:fan@ntu.edu.tw))

### Abstract

A laser measurement system for measuring straightness and parallelism error using a semiconductor laser was proposed. The designing principle of the developed system was analyzed. Addressing at the question of the divergence angle of the semiconductor laser being quite large and the reduction of measurement accuracy caused by the diffraction effect of the light spot at the long working distance, the optical structure of the system was optimized through a series of simulations and experiments. A plano-convex lens was used to collimate the laser beam and concentrate the energy distribution of the diffraction effect. The working distance of the system was increased from 2.6 m to 4.6 m after the optical optimization, and the repeatability of the displacement measurement is kept within 2.2 m in the total measurement range. The performance of the developed system was verified by measuring the straightness of a machine tool through the comparison tests with two commercial multi-degree-of-freedom measurement systems. Two different measurement methods were used to verify the measurement accuracy. The comparison results show that during the straightness measurement of the machine tool, the laser head should be fixed in front of the moving axis, and the sensing part should move with the moving table of the machine tool. Results also show that the measurement error of the straightness measurement is less than 3 m compared with the commercial systems. The developed laser measurement system has the advantages of high precision, long working distance, low cost, and suitability for straightness and parallelism error measurement.

Keywords: straightness, parallelism, laser measurement system, machine tool.

© 2021 Polish Academy of Sciences. All rights reserved

### 1. Introduction

Machine tools are widely used in industry. For machine tools with linear guideways, the measurement of geometric errors originating from assembly processes and manufacturing plays an important role in metrology [1–3]. The parallelism and straightness of a pair of rails are

Copyright © 2021. The Author(s). This is an open-access article distributed under the terms of the Creative Commons Attribution-NonCommercial-NoDerivatives License (CC BY-NC-ND 4.0 <https://creativecommons.org/licenses/by-nc-nd/4.0/>), which permits use, distribution, and reproduction in any medium, provided that the article is properly cited, the use is non-commercial, and no modifications or adaptations are made.

Article history: received December 24, 2020; revised April 12, 2021; accepted April 23, 2021; available online May 25, 2021.

the most basic parameters for machine tools. Several methods are used to obtain a measure of straightness of each rail. Using the granite block and a dial indicator is a common method for geometric error inspection of a linear guideway. However, this method does not obey the “Bryan Principle” during the measuring process and the granite block is heavy and easily scratched. Nowadays, techniques based on different principles for straightness measurements are adopted.

The most common and reliable method for measurement of straightness is based on the interference principle. Chen developed a laser interferometer on the basis of the heterodyne interferometer for measuring the straightness. The standard deviation of the straightness measurement is 0.6  $\mu\text{m}$  and the verified measurement distance is 100 mm [4]. Zhu developed a system for measuring guideway straightness error on the basis of the polarization interference principle. The measuring repeatability of the system is less than 1  $\mu\text{m}$  at a distance of 1,000 mm [5]. Lin developed a laser interferometer for determining the straightness of a moving stage based on the Doppler effect. The repeatability of the interferometer is about 1  $\mu\text{m}$  and the measurement distance is 250 mm [6]. The commercial laser interferometer, such as Renishaw XL-80, can achieve high accuracy measurement with a long working distance. But it is inefficient because only one geometric error can be obtained at one time and the measurement can be easily interrupted when the light source is disturbed.

Another widely used technique for measuring straightness is based on laser alignment. Being compact and easy to use *quadrant detectors/photodetectors* (QD/QPD) and *position sensitive detectors* (PSD) are commonly used in laser alignment systems for high precision measurement of straightness. The different QPD-based MDFM systems have been proposed. Jywe presented an MDFM system that integrated a miniature laser interferometer with a DVD pickup head. The measurement error of straightness is under  $\pm 0.2 \mu\text{m}$  and the measurement distance is 200 mm [7]. Feng developed a compact 6-DOF measurement system using a single-mode fiber-coupled laser for geometric motion errors of the linear guide. The maximum deviation of straightness is 0.5  $\mu\text{m}$  and the verified measurement distance is 650 mm [8]. Liu proposed a straightness measurement system comprising a He–Ne laser and a QPD. The residual error between the HP laser interferometer and the proposed straightness measurement system is less than 0.6  $\mu\text{m}$  and the measuring distance is 200 mm [9]. Fan developed a laser straightness measurement system with an accuracy of 0.3  $\mu\text{m}$  within the range of  $\pm 100 \text{ mm}$ . The repeatability of the system tests was found within 0.5  $\mu\text{m}$  in the total measurement distance of 1000 mm [10]. However, this implementation of QPDs was often used to measure the center of a light spot and, as their response is sensitive to the shape and size of the light spot, they require careful *in situ* calibration.

The PSD-based MDFM systems have also been developed to obtain geometric errors. Hsieh proposed a geometric error measurement system for straightness and parallelism errors. A dual laser interferometer and a PSD were employed in the system. The measurement errors in the horizontal and vertical directions are 0.5  $\mu\text{m}$  and 1.7  $\mu\text{m}$  respectively [11]. Ni developed an MDFM system on the basis of the principle of laser alignment and an autocollimator. The accuracy of measuring straightness error components is better than 1  $\mu\text{m}$  in the measurement range of 500 mm [12]. Rahneberg proposed a 3-DOF measurement system on the basis of a PSD for the straightness measurement. The system utilizes a fiber-coupled laser diode as the light source. The position resolution is 0.1  $\mu\text{m}$  throughout a total distance of 1,000 mm [13].

Some CMOS/CCD sensors are also used to measure straightness based on laser alignment. Chou developed an MDFM system based on a CCD camera. The accuracy of the system in the measurement of the vertical and lateral straightness is within  $\pm 0.5 \mu\text{m}$  in the whole measuring distance of 750 mm [14]. Sun developed a 5-DOF measurement system for motion errors. The straightness error is received by the CMOS camera. The comparison deviation of the horizontal

straightness and the vertical straightness are  $\pm 2.8$  and  $\pm 3.1 \mu\text{m}$  for the measuring distance of 1000 mm [15].

Current straightness measurement methods and techniques mentioned above still have some limitations. Commercial straightness measuring systems for industry such as the API XD 6-D Laser Measurement System and the Renishaw XM-60 Multi-Axis Calibrator have high precision and a long measuring range, however, they are quite expensive. A laser interferometer for error measurement of straightness measurement has the advantage of high accuracy and a long working distance. However, it is relatively big because of the He-Ne laser applied and, again, the laser source is expensive. The implementations of a QD/QPD and a PSD as a sensor to realize the measurement of the straightness errors have the advantage of low cost, compactness, and fast optical adjustment. However, most of the MDFM systems have a limited measuring distance and their accuracy has not been verified at distance exceeding 1500 mm in the literature.

In view of the literature on geometric error measurement systems, in practical applications during the manufacturing and the assembly processes of the machine tools, the developed straightness and parallelism errors measurement system should satisfy the following basic conditions: (1) the measurement process should be as simple as possible; (2) the measuring precision should be reliable; (3) the measurement distance should be longer; (4) the system costs should be lower. Existing developed measurement systems cannot meet all the conditions simultaneously. Considering the problems in actual application, a straightness and parallelism error measurement system using a semiconductor laser was developed with compact structure, low cost, and high precision. The optical measurement principle was analyzed through the Zemax software. The measuring precision was ensured through the calibration tests based on a high-precision 3D nano position stage and the working distance of 4.6 m was verified after the optimization of the light path. The verification experiments of the developed system were conducted by using two different commercial MDFM systems: Renishaw XM-60 Multi-Axis Calibrator and API XD 6-D Laser Measurement System. The parallel error measurement of the guideways was also verified. The developed measurement system can be applied in industry.

## 2. Development of the laser measurement system

Figure 1 presents the schematic of the laser measurement system for straightness and parallelism measurements. The developed measurement system comprises laser-transmitting, pentaprism, and sensing units. In the laser transmitting unit, a semiconductor laser is employed as

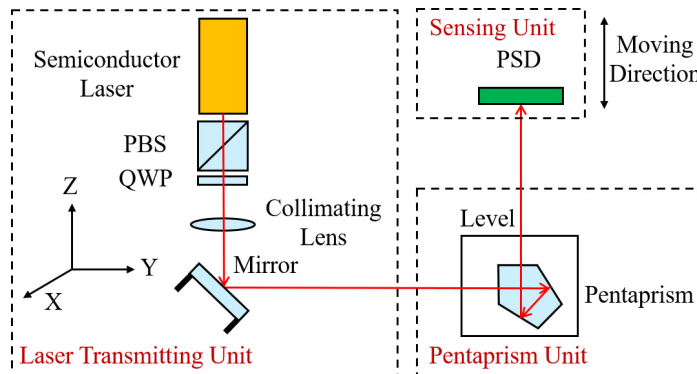


Fig. 1. Diagram of the developed laser measurement system.

the light source. The laser beam passes through a *polarized beam splitter* (PBS) and a *quarter waveplate* (QWP), and is then collimated by a plano-convex lens. The collimated light beam is next reflected by a plane mirror. The mirror is mounted onto a commercial 2D-angle steering mechanism to adjust the reflect beam angle in line with the moving axis of the guideway. The reflected beam will pass through a pentaprism and then project onto the sensing surface of a PSD (S5990-01 Hamamatsu; active area:  $4 \times 4$  mm; position resolution:  $0.7 \mu\text{m}$ ) mounted inside the sensing unit to detect the horizontal and vertical straightness errors of the detected target. When the sensing unit moves along the linear guideway, the position deviation of the guideway in the horizontal and vertical directions will cause a relative change in the position of the light spot received by the PSD.

## 2.1. Straightness measurement

When the photosensitive surface of the PSD is illuminated by a light spot, the resulting photocurrents to the electrodes are changed with the position of the received spot. From these photocurrents the normalized  $y$  and  $z$  outputs can be found from the following equations:

$$y = k_y \times \frac{(I_2 + I_3) - (I_1 + I_4)}{I_1 + I_2 + I_3 + I_4 + I_b} \times \frac{L}{2}, \quad (1)$$

$$z = k_z \times \frac{(I_2 + I_4) - (I_1 + I_3)}{I_1 + I_2 + I_3 + I_4 + I_b} \times \frac{L}{2}, \quad (2)$$

where  $y$  and  $z$  are the position coordinates of the light spot;  $I_i$  is the photocurrent to electrode  $i$  of the PSD ( $i = 1, 2, 3, 4$ );  $I_b$  is the output current of the PSD caused by background light;  $L$  is the side length of the sensing surface of the PSD;  $k_i$  is the coefficient which can be obtained by the calibration experiments.

According to (1) and (2), when the intensity of the background light is the same, the stronger the laser intensity the higher the PSD sensitivity and accuracy will be. The output current of each electrode of the PSD is also affected by the shape and size of the light spot. The divergence angle of the laser should be small so that a round and symmetric spot can be obtained to improve the sensitivity of the PSD.

## 2.2. Parallelism measurement

In the parallelism measurement of two parallel guideways, two perfectly parallel laser beams aligned to the guideways are required for measurement reference. This is done by moving the laser beam (moving the pentaprism) from the first guideway to the second guideway after the first guideway measurement is performed. During the laser beam transfer, the pitch and roll positions of the pentaprism will affect the alignment of the laser. The pitch and roll positions of the pentaprism should be preserved through a dual-axis level integrated with pentaprism during the assembly.

Figure 2 shows the schematic of the parallelism measurement setup. The laser is constructed with the laser beam aligned in the horizontal plane and perpendicular to the guideways. The pentaprism is placed in the laser beam path, bending the beam 90 degrees along the length of the linear guideway. As the laser beam exits the pentaprism, it is aligned parallel to the first rail through adjusting the laser and the pentaprism. When moving the pentaprism from the first guideway position to the second guideway position, the adjustment is guided by a dual-level sensor [16] integrated to the pentaprism assembly so that its pitch and roll positions are identical

to its first guideway position. In result, a laser beam direction the same as for the first rail is established. The parallelism errors between two guideways can be obtained according to the straightness of each guideway calculated by (1) and (2).

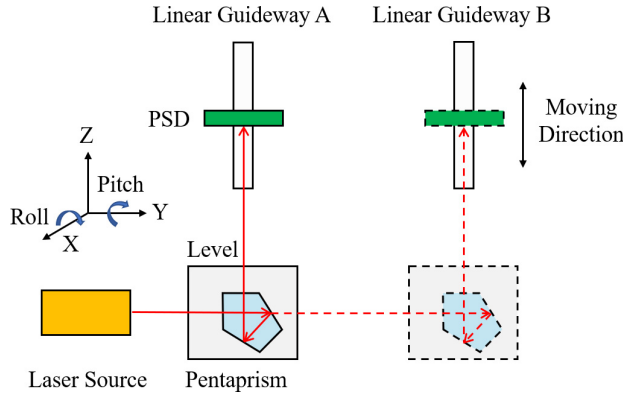


Fig. 2. Diagram of the parallelism measurement setup.

### 3. Analysis on the collimating lens and the diffraction effect of the light spot

As described in the previous section, a semiconductor laser (whose detailed parameters are listed in Table 1) is employed as the light source in the developed laser measurement system owing to its advantages of small size and low cost. However, the divergence angle is larger than the stabilized lasers (single/dual-frequency laser), such as the He–Ne laser. In practical application, the spot of the incident light always has a certain shape and size. A circular aperture is usually attached to ensure the beam quality so that the semiconductor laser can have a round spot.

Table 1. The parameters of the semiconductor laser.

Parameter	Value
Wavelength	635 nm
Exit pupil power	5 mW
Divergence angle	0.6 mrad
Optical system	Optically coated glass lens
Fiber core diameter	Single mode 4 $\mu\text{m}$
Working voltage	DC 5 V

Considering that the distance between the aperture and the PSD is much larger than the size of the aperture, according to the far-field condition of the circular Fraunhofer diffraction [17], the minimum distance that diffraction occurs (the distance between the aperture and the PSD) can be obtained by (3):

$$|z_0| \gg \frac{kr^2}{2\pi} = \frac{r^2}{\lambda}, \quad (3)$$

where  $z_0$  is the minimum distance between the aperture and the PSD;  $r$  is the radius of the aperture;  $\lambda$  is the wavelength of the light beam;  $k$  is the wave number ( $k = 2\pi/\lambda$ ).

From (3) the minimum distance  $z_0$  can be calculated as 0.89 m ( $r = 0.75$  mm,  $\lambda = 635$  nm). Once the distance between the aperture and the PSD is larger than 0.89 m, the light spot detected on the sensing surface of the PSD will be a diffraction ring centered on the Airy disk rather than one bright light as shown in Fig. 3.

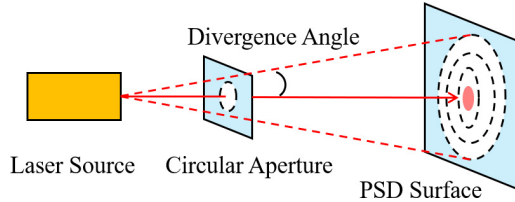


Fig. 3. Light spot detected on the PSD surface.

Figure 4 shows the circular aperture Fraunhofer diffraction phenomenon observed in the actual measurement when the distance between the aperture and the PSD surface is 4 m (the laser wavelength is 635 nm and the diameter of the circular aperture is 1.5 mm). The detected signal of the PSD is related to the center position of the light spot energy. The diffraction will cause the redistribution of the light intensity projected on the sensing surface of the PSD, which will cause the reduction of the measurement accuracy of the PSD. The most significant impact is that the repeatability of the measuring system will be reduced. In practical application, the repeatability of the MDFM system is one of the most important measures of whether the instrument is reliable. A simple and direct proof test about the adverse effect of the diffraction phenomenon on the developed laser measurement system can be seen in Figs. 5a and b. Figure 5 shows the repeatability of the straightness measurement when the diffraction occurs (laser working distance: 4 m–4.6 m) and does not occur (laser working distance: 2 m–2.6 m). Figure 5 displays that the repeatability of the laser measurement system is poor when the diffraction occurs.

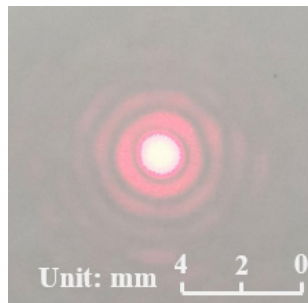


Fig. 4. Observed diffraction phenomenon.

Suppose that Airy disk is in the center of the sensing surface of the PSD, the light intensity at any point on the sensitive surface of the PSD can be obtained as:

$$I_p = A_0 \left[ 1 - \frac{1}{2}m^2 + \frac{1}{3} \left( \frac{m^2}{2!} \right)^2 - \frac{1}{4} \left( \frac{m^3}{3!} \right)^3 + \frac{1}{5} \left( \frac{m^4}{4!} \right)^4 + \dots \right], \quad (4)$$

where  $m = (\pi R \sin \theta)/\lambda$ ;  $R$  is the radius of the aperture;  $\theta$  is the field angle between the spot edge and the center of the circular aperture.

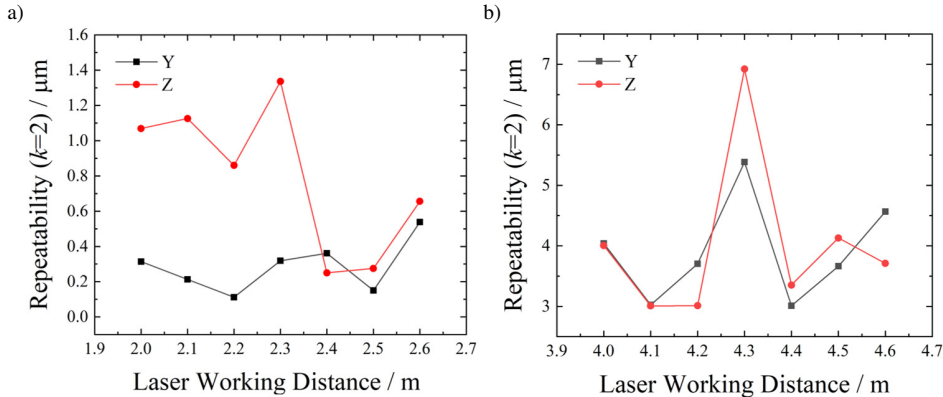


Fig. 5. Repeatability of the straightness measurement when: a) diffraction does not occur; b) diffraction occurs.

According to the first-order Bessel function, (3) can be expressed as:

$$I_p = A_0^2 \frac{J_1^2\left(\frac{2\pi R \sin \theta}{\lambda}\right)}{\left(\frac{\pi R \sin \theta}{\lambda}\right)^2} = A_0^2 \frac{J_1^2(2m)}{m^2} = I_0 \frac{J_1^2(2m)}{m^2}, \quad (5)$$

where  $J_1$  is the Bessel function of the first kind.

To simplify the analysis process, the bright fringes with concentrated energy in the diffraction distribution can be regarded as circular ring lines with no width and uniform energy distribution. According to (4) and (5), the diffraction intensity and energy distribution of each level of the diffraction ring can be obtained as shown in Table 2, where  $R = 1$  mm and  $\lambda = 635$  nm.

Table 2. Diffraction light intensity and energy distribution of the circular hole Fraunhofer diffraction.

Fringe Order	2 m	$\theta ["]$	Energy Distribution %
Airy Disk	0	0	83.78
1 <sup>st</sup> order min	3.83	138	0
1 <sup>st</sup> order max	5.15	186	7.22
2 <sup>nd</sup> order min	7.02	252	0
2 <sup>nd</sup> order max	8.41	303	2.77
3 <sup>rd</sup> order min	10.17	367	0
3 <sup>rd</sup> order max	11.60	418	1.62

Table 1 shows that in the circular hole Fraunhofer diffraction, the light energy of Airy spot accounts for 84% of the entire incident light energy. The spot size of the circular hole Fraunhofer diffraction is inversely proportional to the radius of the circular aperture and proportional to the laser wavelength. The smaller the radius of the circular hole, the longer the wavelength, the more obvious the diffraction phenomenon, and the greater the impact on the output of the PSD. To increase the measurement accuracy of the developed system, a concentrated light beam is preferred.

The sensing accuracy of the PSD can be increased by improving the quality of the laser beam. This can be done by using a plano-convex lens as the collimator objective in the collimator unit. Figure 6 shows the simulation results of the collimation effect at different focal lengths and the diffraction phenomenon when the focal lengths changes. Parameters employed in the simulations are summarized in Table 3. Figure 6 shows that the energy distribution of the diffraction ring is concentrated in the central area when using a plano-convex lens.

Table 3. Diffraction light intensity and energy distribution of the circular hole Fraunhofer diffraction.

Parameter	Value
Wavelength	635 nm
Divergence angle	0.6 mrad
Aperture diameter	1.5 mm
Focal length of the collimator objective	1 m, 2 m
Distance between the laser and the PSD surface	4 m
Distance between aperture and lens	3 cm

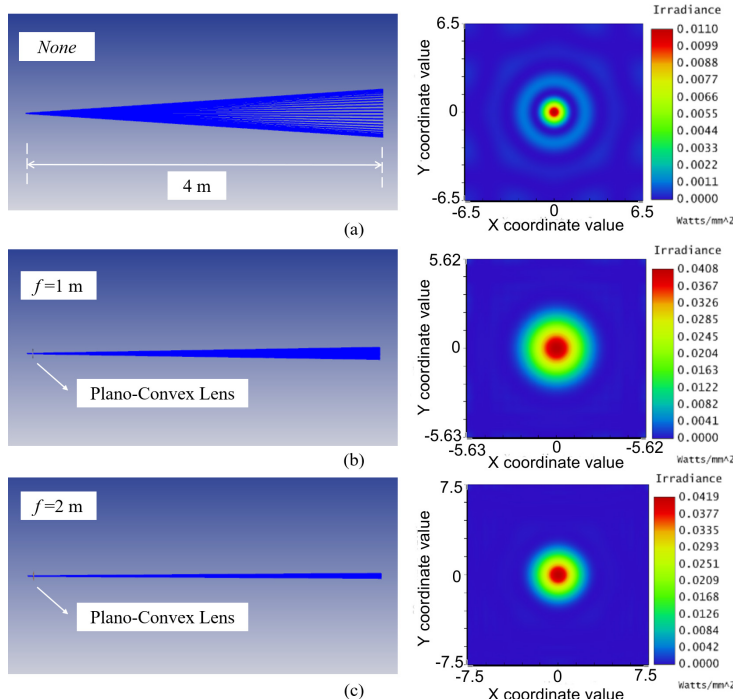


Fig. 6. Schematic of the optical simulations: a) without a collimator, b) with a collimator  $f = 1$  m, c) with a collimator  $f = 2$  m.

The feasibility of the simulation results was verified through some experiments. The influences of the focal length and the light intensity attenuation were also investigated. A laser beam with a wavelength of 635 nm emitted from the semiconductor passed through a circular aperture and then was collimated by using a plano-convex lens. At the beginning of the experiment, the sensing

unit was set in a guideway, the laser beam from the semiconductor was adjusted to project on the sensing surface of the PSD in the sensing unit. Both the sensing unit and the guideway were driven by a servo motor, the total moving distance is 4.6 m and the moving interval was 10 cm. When the sensing unit arrived at the measuring point, the output signals of the PSD were recorded. The total measurement process was repeated for 5 times, and then the repeatability of each measuring point was calculated. Figure 7 shows the repeatability results of the straightness measurements for five times under different optical structures. The plano-convex lens can improve the quality of the light spot, and using a plano-convex lens with a focal length of 2 m can improve the measurement repeatability significantly for the 4.6 m working distance. Figure 8 shows the repeatability of the straightness measurement after the optical path is collimated through the plano-convex lens

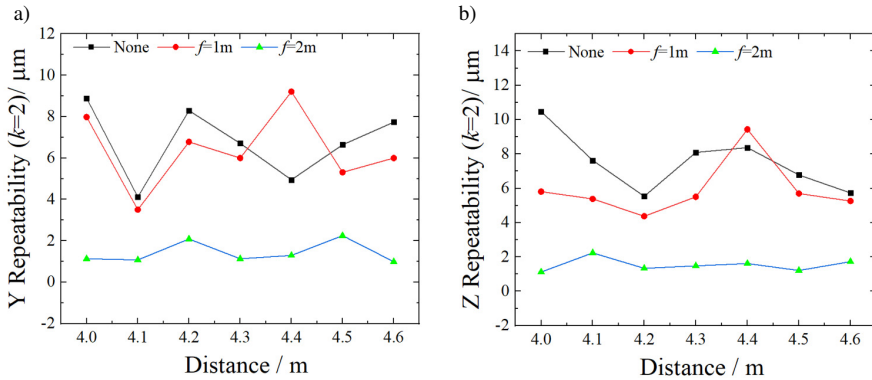


Fig. 7. Repeatability results under different optical structures and parameters: a) Y repeatability; b) Z repeatability.

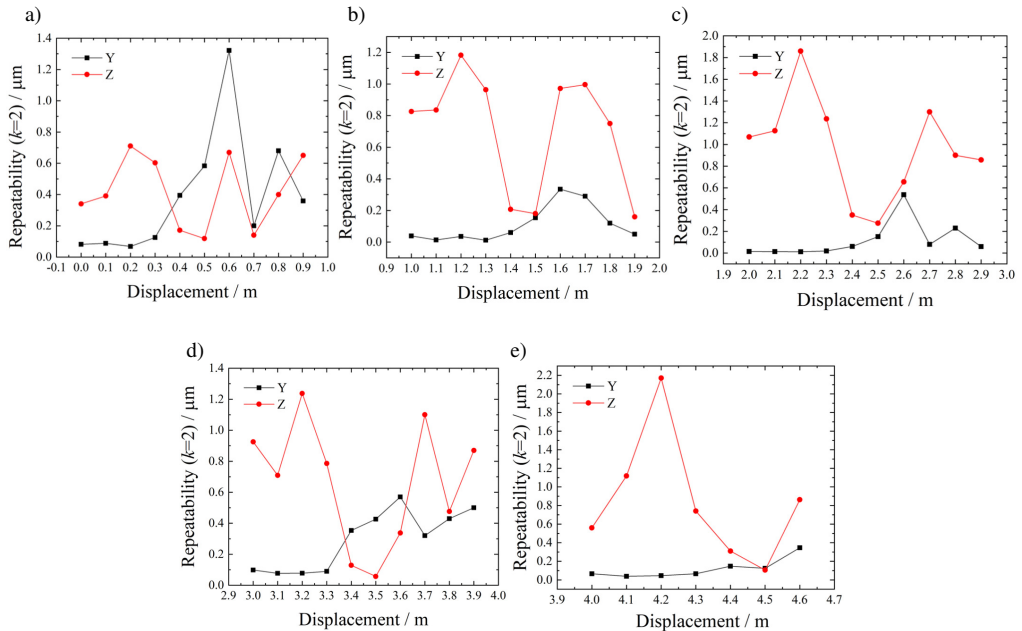


Fig. 8. Repeatability of the straightness measurement in the total measurement range of 4.6 m:  
 a) 0–0.9 m; b) 1–1.9 m; c) 2–2.9 m; d) 3–3.9 m; e) 4–4.6 m.

( $f = 2$  m). The repeatability of the displacement measurement is kept within 2.2  $\mu\text{m}$  in the total measurement range of 4.6 m.

#### 4. Precision calibration

According to (1) and (2), the parameters  $k_y$  and  $k_z$  can be calibrated with a series of certain offset displacement Y and Z values measured by the designed experimental setup. Figure 9 displays that the calibration tests for straightness errors were carried out with a high-precision 3D nano position stage (PI, model P561.3 CD, with a repeatability of 2 nm and a distance of 100  $\mu\text{m}$  in each direction, Physik Instrumente Co. Ltd., Germany). In the calibration process, the sensing part was mounted on the PI stage, which was driven by a servo motor along the X axis. The motion distance was 460 cm with a step of 5 cm. The linear motor was driven to shift the PI stage, after the adjustment of the light path (ensure that the optical measuring axis was in line with the moving axis), the PI stage was moved within a range from  $-100 \mu\text{m}$  to  $+100 \mu\text{m}$ , at an approximate increment of 10  $\mu\text{m}$  along the Y and Z axes, respectively. The output signals were recorded every time when the PI stage was controlled to provide standard displacement. The measurement was performed five times for forward and backward directions. Figures 10a and

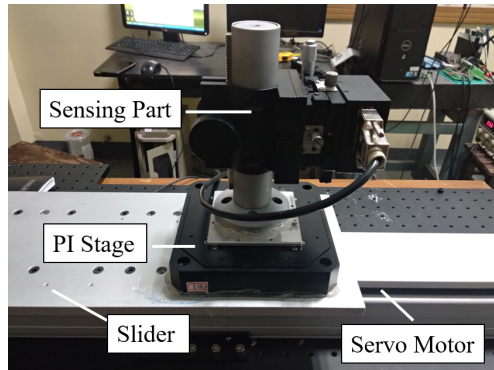


Fig. 9. Calibration test setup.

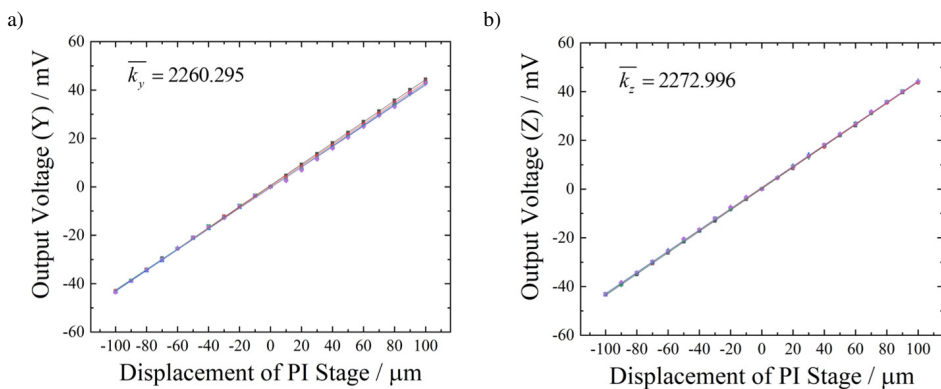


Fig. 10. Corresponding fitting curve of experimental data when the moving distance is 5 cm:  
a) Y output voltage; b) Z output voltage.

10b show the corresponding fitting curve of the experimental data on the basis of the least-square method when the moving distance of the linear motor is 5 cm. Calibration results show that the relationship between the straightness error and the output signals is linear. They also show that the range of measurement can reach  $\pm 100 \mu\text{m}$ .

Parameter  $k_i$  is obtained with the fitting curves when it is equal to 2260.295 and  $k_z$  is equal to 2272.996 when the moving distance is 5 cm. Although the optical path is collimated, the shape and size of the light spot can still change along the measurement path. Parameter  $k_i$  varies at different laser working distances as shown in Fig. 11. Once the size of the detected light spot exceeds the sensing area of the PSD during the calibration process, the output of the PSD is nonlinear. This can explain why the calibration coefficients change rapidly when the laser working distance is longer than 250 cm.

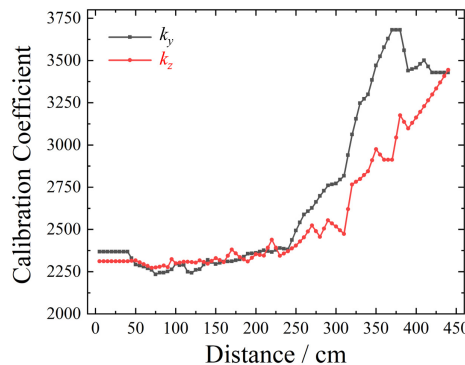


Fig. 11. Calibration coefficients for different laser working distances.

After the calibration experiments, all the calibration coefficients are stored in the system software, and the system can choose the right coefficient according to the measurement distance automatically (the measurement distance and the moving interval should be fed into the software first before the measurement). The laser path is strictly parallel to the moving axis during the calibration process, so the recalibration of the parameter is unnecessary before every new measurement. In the actual measurement, the position of the sensing part must be recorded and the correct parameter corresponding to each distance must be chosen to perform efficient and precise measurements with reliability.

## 5. Verification and application of the straightness and parallelism measurements

The verification of the straightness of the proposed system was conducted by using two different commercial laser interferometers: a Renishaw XM-60 Multi-Axis Calibrator and an API XD 6-D Laser Measurement System as reference standards to measure straightness errors of the three-axis machine tool with the measurement distance of 700 mm. Figure 12 shows the detected machine tool. During the measurement of straightness of the machine tool, according to the user's manual the similarity of these commercial MDFM systems is that the laser head should be fixed on the machine bed while the sensor is mounted to the machine spindle as shown in Fig. 13.

During the straightness measurement, the reference axis of the laser beam will change its position because of the pitch and yaw errors of the machine bed and there a problem arises of cross-talk error. The proper way to measure the straightness errors should be that the laser head



Fig. 12. Detected machine tool.

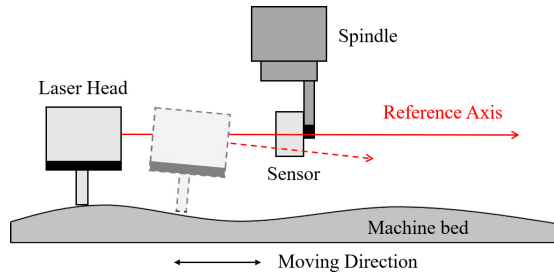


Fig. 13. Setup of the commercial MDFM system.

is fixed in front of the moving axis and the sensing part moves with the moving table as shown in Fig. 14.

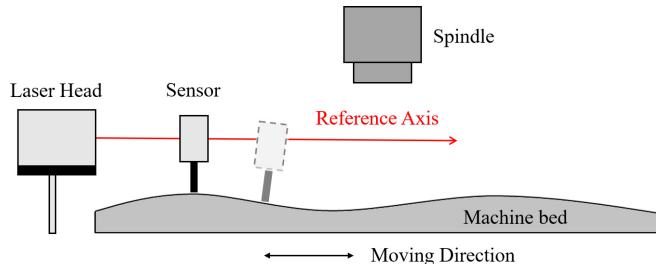


Fig. 14. Setup of the proper way of measuring the straightness errors of a machine tool.

Figure 15 shows the position change of the light spot projected on the PSD surface in these two cases. Assuming that the light spot projects on the center of the PSD surface at the very beginning of the measurement. When the laser head moves along with the machine bed, the angular error of the machine bed will cause changes in the optical path as shown in Fig. 15a. The position change of the light spot  $\Delta d_1$  can be expressed as:

$$\Delta d_1 = D \tan \theta, \quad (6)$$

where  $D$  is the distance between the laser head and PSD surface;  $\theta$  is the angular error (pitch or yaw) of the machine bed during the movement.

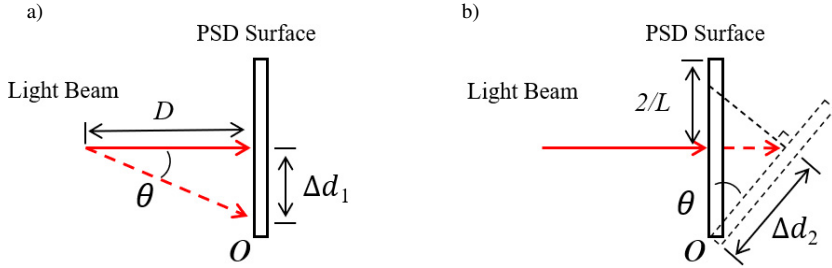


Fig. 15. Position change of the light spot projected on the PSD surface in two cases: a) the laser head is moving, b) the laser head is fixed.

When the laser head is fixed and the sensing part moves with the machine bed, the position change of the light spot  $\Delta d_2$  as shown in Fig. 15b can be expressed as:

$$\Delta d_2 = H - \frac{L}{2} = \frac{L}{2 \cos \theta} - \frac{L}{2} = \frac{L}{2} \left( \frac{1}{\cos \theta} - 1 \right), \quad (7)$$

where  $L$  is the side length of the sensing surface of the PSD.

From Eqs. (6) and (7) we can see that the output signal of the PSD is different in the two cases. If  $D=2\text{m}$ ,  $\theta=1''$ ,  $L=4\text{ mm}$ , the position change of the light spot  $\Delta d_1$  and  $\Delta d_2$  can be calculated, which are  $\Delta d_1=9.69\text{ }\mu\text{m}$  and  $\Delta d_2=2.35\times 10^{-8}\text{ }\mu\text{m}$ , respectively. The differences in measurement errors in these two cases can reach nearly  $10\text{ }\mu\text{m}$ .

Figure 16 shows the comparison testing setup of the straightness errors of the machine tool between the developed laser measurement system and two commercial MDFM systems. Each commercial MDFM system was assembled in two ways. The first one is that the laser head is fixed on the machine bed while the sensor is mounted to the machine spindle, the second one is that the laser head is fixed in front of the moving axis and the sensing part moves with the moving table. Figure 17a shows the straightness measurement results while the laser head is moving. The straightness results obtained by Renishaw and API through the same measuring method (the laser head moving) are different as shown in Fig. 17a. This is because both sensors are not placed in the same position due to the limitations of each adjustment mechanism. Figures 17b and 17c show the measurement results while the laser head is not moving. When both sensors (Renishaw and API) are placed in the same position, the measurement results are almost the same. Figures 17b and 17c

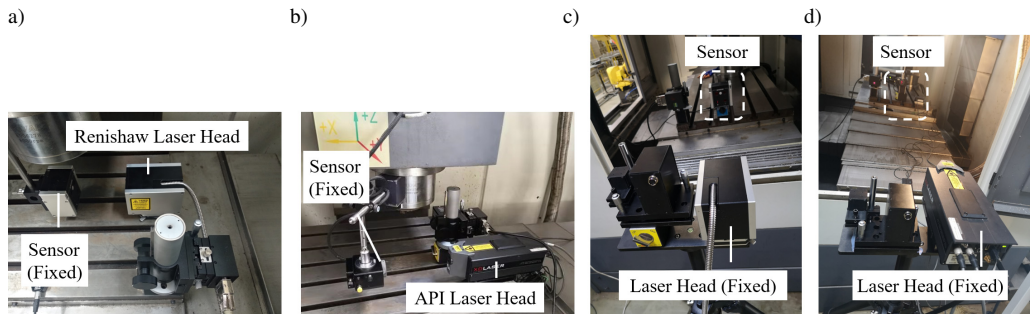


Fig. 16. Comparison testing of the straightness errors in two different ways: a) Renishaw laser head fixed; b) API laser head fixed; c) Renishaw laser head moving; d) API laser head moving.

also show that compared with two commercial MDFM systems, the measurement errors of the developed system are no more than 3  $\mu\text{m}$ . This error is within the acceptable range because the position of the sensors of both measuring systems is not exactly the same. It can be compensated with an error separation method.

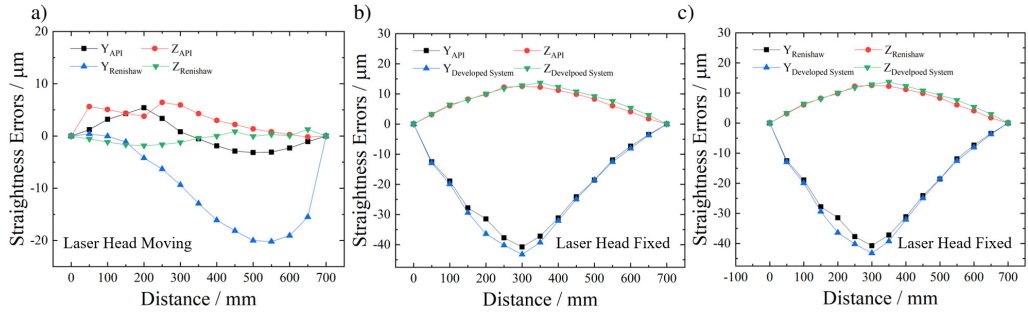


Fig. 17. Straightness measurement results: a) Renishaw and API; b) Renishaw and the developed system; c) API and the developed system.

Figure 18 shows the repeatability of the straightness measurements results for five times. The maximum measurement repeatability of Renishaw and API MDFM system is 4.5  $\mu\text{m}$ , the maximum repeatability of the developed system is 3  $\mu\text{m}$ . Compared with the commercial MDFM systems, the developed system has higher accuracy and was much cheaper to build.

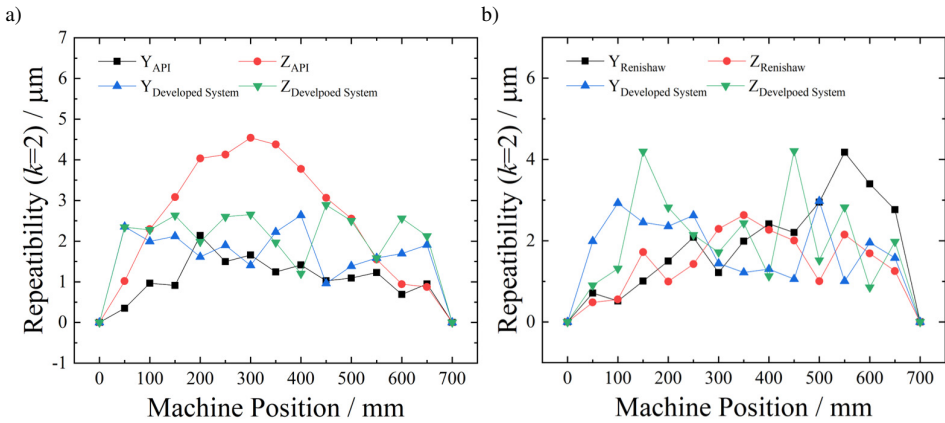


Fig. 18. Repeatability of the straightness measurements results for five times: a) API and the developed system; b) Renishaw and the developed system.

The verification of the proposed laser measurement system was also conducted by measuring the parallelism of two parallel linear guideways as shown in Fig. 19. In this case, the total measurement range was 1,400 mm. Figure 20 presents the measurement results. The measured results can help to adjust the accuracy of both guide rails during the assembly.

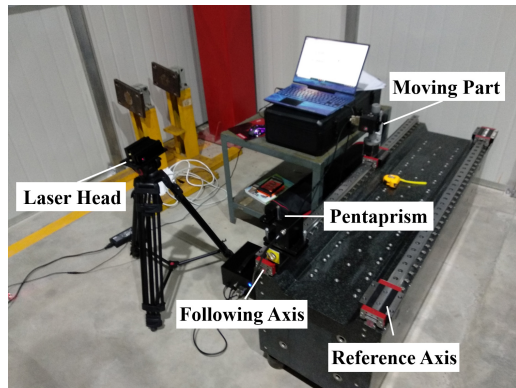


Fig. 19. Parallel error measurement of guideways.

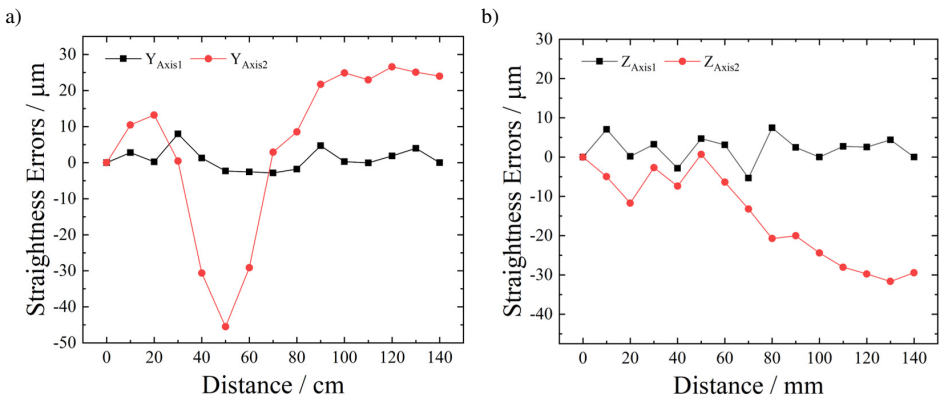


Fig. 20. Measurement results: a) Y direction; b) Z direction.

## 6. Conclusions

In this study, a compact laser measurement system for straightness and parallelism measurement is proposed. Compared with commercial MDFM systems, our proposed laser measurement system can reach high accuracy at a rather low cost. A semiconductor laser was used as the light source. Aiming to reduce the divergence angle of the semiconductor laser and the diffraction effect of the light spot, a plano-convex lens was used to collimate the laser beam. The working distance of 4.6 m was verified after the optical optimization, and the repeatability of the displacement measurement is kept within 2.2  $\mu\text{m}$  in the total measurement range. A high-precision 3D nano position stage was used for the calibration tests. The verification of the straightness of the proposed system was conducted by using two different commercial laser interferometers: a Renishaw XM-60 Multi-Axis Calibrator and an API XD 6-D Laser Measurement System. The comparison results show that during the straightness measurement process in a machine tool, the laser head should be placed in front of the moving axis, and the sensing part should move with the moving table of the machine tool. Compared with the existing geometric error measurement system, the developed laser measurement system has the advantages of low cost and long working distance, and as such it can be applied in industry. We intend the proposed system to be a component

in a 6-DOF measurement system. Our future work will focus on integrating the angle (pitch, yaw, and roll) measurement and positioning function. An improvement of the error compensation method is also desirable.

### Acknowledgement

This research was funded by the National Key R&D Program of China under Grant no. 2019YFB2004901.

### References

- [1] Schwenke, H., Knapp, W., & Haitjema, H. (2008). Geometric error measurement and compensation of machines – an update. *CIRP Annals*, 57(2), 660–675. <https://doi.org/10.1016/j.cirp.2008.09.008>
- [2] Chen, Z., & Liu, X. (2020). A Self-adaptive interpolation method for sinusoidal sensors. *IEEE Transactions on Instrumentation and Measurement*, 69(10), 7675–7682. <https://doi.org/10.1109/TIM.2020.2983094>
- [3] Acosta, D., & Albajez, J. A. (2018). Verification of machine tools using multilateration and a geometrical approach. *Nanomanufacturing and Metrology*, 1(1), 39–44. <https://doi.org/10.1007/s41871-018-0006-y>
- [4] Chen, B. Y., Zhang, E. Z., & Yan, L. P. (2009). A laser interferometer for measuring straightness and its position based on heterodyne interferometry. *Review of Scientific Instruments*, 80(11), 115113. <https://doi.org/10.1063/1.3266966>
- [5] Zhu, L. J., Li, L., Liu, & J. H. (2009). A method for measuring the guideway straightness error based on polarized interference principle. *International Journal of Machine Tools and Manufacture*, 49(3–4), 285–290. <https://doi.org/10.1016/j.ijmachtools.2008.10.009>
- [6] Lin, S. T. (2001). A laser interferometer for measuring straightness. *Optics & Laser Technology*, 33(3), 195–199. [https://doi.org/10.1016/S0030-3992\(01\)00024-X](https://doi.org/10.1016/S0030-3992(01)00024-X)
- [7] Jywe, W. Y., Liu, C. H., Shien, W. H., Shyu, L. H., & Fang, T. H. (2006). Development of a multi-degree of freedoms measuring system and an error compensation technique for machine tools. *Journal of Physics Conference Series*, 48(1), 761–765. <https://doi.org/10.1088/1742-6596/48/1/144>
- [8] Feng, Q. B., Zhang, B. & Cui, C. X. (2013). Development of a simple system for simultaneous measuring 6DOF geometric motion errors of a linear guide. *Optics Express*, 21(22), 25805–25819. <https://doi.org/10.1364/OE.21.025805>
- [9] Liu, C. H., Chen, J. H., & Teng, Y. F. (2009). Development of a straightness measurement and compensation system with multiple right-angle reflectors and a lead zirconate titanate-based compensation stage. *Review of Scientific Instruments*, 80(11), 115105. <https://doi.org/10.1063/1.3254018>
- [10] Fan, K. C. (2000). A laser straightness measurement system using optical fiber and modulation techniques. *International Journal of Machine Tools Manufacture*, 40(14), 2073–2081. [https://doi.org/10.1016/S0890-6955\(00\)00040-7](https://doi.org/10.1016/S0890-6955(00)00040-7)
- [11] Hsieh, T. H., Chen, P. Y., & Jywe, W. Y. (2019). A geometric error measurement system for linear guideway assembly and calibration. *Applied Sciences*, 9(3), 574. <https://doi.org/10.3390/app9030574>
- [12] Ni, J., & Huang, P. S. (1992). A multi-degree-of-freedom measuring system for CMM geometric errors. *Journal of Manufacturing Science and Engineering*, 114(3), 362–369. <https://doi.org/10.1115/1.2899804>
- [13] Rahneberg, I., & Büchner, H. J. (2009). Optical system for the simultaneous measurement of two-dimensional straightness errors and the roll angle. *Proceedings of the International Society for Optics and Photonics*, the Czech Republic, 7356. <https://doi.org/10.1117/12.820634>

- [14] Chou, C., Chou, L. Y. & Peng, C. K. (1997). CCD-based CMM geometrical error measurement using Fourier phase shift algorithm. *International Journal of Machine Tools and Manufacture*, 37(5): 579–590. [https://doi.org/10.1016/S0890-6955\(96\)00078-8](https://doi.org/10.1016/S0890-6955(96)00078-8)
- [15] Sun, C., Cai, S., & Liu, Y. (2020). Compact laser collimation system for simultaneous measurement of five-degree-of-freedom motion errors. *Applied Sciences*, 10(15), 5057. <https://doi.org/10.3390/app10155057>
- [16] Huang, Y., Fan, Y., Lou, Z., Fan, K. C., & Sun, W. (2020). An innovative dual-axis precision level based on light transmission and refraction for angle measurement. *Applied Sciences*, 10(17), 6019. <https://doi.org/10.3390/app10176019>
- [17] Born M., & Wolf E. (2013). *Principles of Optics: Electromagnetic Theory of Propagation, Interference and Diffraction of Light*. Elsevier. <https://www.sciencedirect.com/book/9780080264820/principles-of-optic>



**Peng Xu** was born in inner Mongolia, China in 1994. He is currently a Ph.D. student in the Nano Measurement Laboratory, Hefei University of Technology. His research interests include precision measurement technology and system. He is specifically engaged in development of micro probes for micro/nano CMMs.



**Rui-Jun Li** received his Ph.D. degree in precision instrumentation and mechanics from Hefei University of Technology, Hefei, China, in 2013. He is currently Full Professor and Head of the Nano Measurement Laboratory at Hefei University of Technology. He has published more than 50 papers. His research activity focuses on precision engineering, micro/nano measurement, photo-electrical inspection, and CMMs.